Published in final edited form as:
Sci Signal. ; 8(398): ra101. doi:10.1126/scisignal.aaa7677.

The Golgi apparatus is a functionally distinct Ca^{2+} store regulated by PKA and Epac branches of the β_1-adrenergic signaling pathway

Zhaokang. Yang[1,*], **Hannah M. Kirton**[1], **David A. MacDougall**[1], **John P. Boyle**[2], **James Deuchars**[1], **Brenda Frater**[1], **Sreenivasan Ponnambalam**[3], **Matthew E. Hardy**[1], **Edward White**[1], **Sarah C. Calaghan**[1], **Chris Peers**[2], and **Derek S. Steele**[1,*]

[1]School of Biomedical Sciences, University of Leeds, Leeds, UK England, LS29JT

[2]Leeds Institute of Cardiovascular and Metabolic Medicine, University of Leeds, Leeds, UK England, LS29JT

[3]School of Molecular and Cellular Biology, University of Leeds, Leeds, UK England, LS29JT

Abstract

Ca^{2+} release from the Golgi apparatus regulates key functions of the organelle, including vesicle trafficking. However, the signaling pathways that control this form of Ca^{2+} release are poorly understood and evidence of discrete Golgi Ca^{2+} release events is lacking. Here, we identified the Golgi apparatus as the source of prolonged Ca^{2+} release events that originate from the nuclear 'poles' of primary cardiac cells. Once initiated, Golgi Ca^{2+} release was unaffected by global depletion of sarcoplasmic reticulum Ca^{2+}, and disruption of the Golgi apparatus abolished Golgi Ca^{2+} release without affecting sarcoplasmic reticulum function, suggesting functional and anatomical independence of Golgi and sarcoplasmic reticulum Ca^{2+} stores. Maximal activation of β_1-adrenoceptors had only a small stimulating effect on Golgi Ca^{2+} release. However, inhibition of phosphodiesterase (PDE) 3 or 4, or downregulation of PDE 3 and 4 in heart failure markedly potentiated β_1-adrenergic stimulation of Golgi Ca^{2+} release, consistent with compartmentalization of cAMP signaling within the Golgi apparatus microenvironment. β_1-adrenergic stimulation of Golgi Ca^{2+} release involved activation of both Epac and PKA signaling pathways and CaMKII. Interventions that stimulated Golgi Ca^{2+} release induced trafficking of vascular growth factor receptor-1 (VEGFR-1) from the Golgi apparatus to the surface membrane. These data establish the Golgi apparatus as a juxtanuclear focal point for Ca^{2+} and β_1-adrenergic signaling, which functions independently from the sarcoplasmic reticulum and the global Ca^{2+} transients that underlie the primary contractile function of the cell.

[*]To whom correspondence should be addressed: d.steele@leeds.ac.uk.

Author contributions: Yang: confocal Ca^{2+} imaging and DAF-2 experiments; Kirton: Ca^{2+} imaging and immunofluorescence experiments. MacDougall: Western blot analysis; Boyle: Immunofluorescence measurements; Deuchars: electron microscopy; Frater: electron microscopy; Ponnambalan immunofluorescence experiments and experimental design; Hardy: preparation of heart failure model; White: preparation of heart failure model; Calaghan Western blot analysis and experimental design; Peers: experimental design, immunofluorescence and editing of draft manuscript; Steele: Experimental design, manuscript preparation and overall project management.

Competing interests: The authors declare that they have no competing interests.

Europe PMC Funders Author Manuscripts

Introduction

The Golgi apparatus has an integral role in the modification, sorting and packaging of macromolecules originating from the rough endoplasmic reticulum (ER), vesicular transport of secreted lipids, proteins and carbohydrates, and the formation of lysosomes1. Previous findings have shown that Ca^{2+} within the Golgi apparatus can regulate both its structure and function. For example, reduced Golgi Ca^{2+} uptake was associated with changes in structure, protein sorting and vesicle trafficking2,3. It has also been suggested that localized increases in cytosolic Ca^{2+} concentration due to Golgi Ca^{2+} release control vesicle fusion and cargo transport3–5. This is supported by work identifying Ca^{2+} binding proteins associated with the Golgi membrane, which transduce local cytosolic Ca^{2+} signals into regulatory events6. However, relatively little is known about the role of the Golgi apparatus as a Ca^{2+} signaling organelle or the pathways that regulate Golgi Ca^{2+} release.

The Ca^{2+} concentration gradient across the Golgi apparatus membrane is generated by the secretory pathway Ca^{2+} ATPase1 (SPCA1)2,7,8 and SERCA9–11. Ca^{2+} binding proteins within the Golgi lumen, such as calnuc, increase the Ca^{2+} storage capacity of the organelle in a manner analogous to calsequestrin in the SR/ER12. Most previous studies have concluded that inositol 1,4,5-trisphosphate ($InsP_3$) receptors ($InsP_3Rs$) mediate Golgi Ca^{2+} efflux3,13–15. However, this is based on data from cell lines, where the $InsP_3$ Ca^{2+} signaling is dominant. In neonatal cardiac myocytes, *trans* Golgi apparatus Ca^{2+} depletion occurs in response to agonists of the ryanodine receptor (RyR), but not the $InsP_3R^2$, indicating that Golgi Ca^{2+} regulation exhibits cell type specialization.

The Golgi apparatus Ca^{2+} efflux mechanism has been studied indirectly by targeting Ca^{2+} probes to the lumen of the organelle8,13,14,16, or by using selective disrupting agents to assess its contribution to cytosolic Ca^{2+} transients8,17,18. However, direct evidence of Ca^{2+}-release events originating from the Golgi apparatus is lacking; it is possible that in cells that exhibit large ER/SR cytosolic Ca^{2+} transients, Golgi Ca^{2+} efflux may be obscured. Alternatively, by virtue of its location, the organelle might dictate local Ca^{2+} signaling despite global cytosolic Ca^{2+} transients; the Golgi apparatus typically appears as a continuous ribbon of flattened stacks, either encircling or adjacent to the nucleus2,19. Released Ca^{2+} may, therefore, have privileged access both to the Golgi apparatus microenvironment and the nucleoplasm.

The aim of the present study was to establish whether Golgi Ca^{2+}-release events can be identified in cells that exhibit large cytosolic ER/SR derived Ca^{2+} transients and if present, to characterize the signaling pathways that control Ca^{2+}-release from the organelle. Our findings establish the Golgi apparatus as a nexus for β_1-adrenergic signaling and demonstrate its capacity to dictate the local Ca^{2+} concentration within the Golgi microenvironment, with consequent effects on protein trafficking in primary cardiac cells.

Results

Prolonged Ca^{2+}-release events occur at the nuclear poles

Experiments were carried out to detect changes in local Ca^{2+}-release in the vicinity of the Golgi apparatus and associated nuclei. Sequential x-y images obtained from a fluo-4 loaded adult rat ventricular myocyte (ARVM) with the confocal plane adjusted such that one of the 2 nuclei was in sharp focus is shown (Fig. 1*A*). A localized Ca^{2+}-release event is apparent at the lower 'nuclear pole'. Subsequent frames (Fig. 1A, *upper right*) and corresponding surface plots (Fig. 1A, *lower right*) reveal a prolonged elevation of nucleoplasmic Ca^{2+} concentration. In line-scan images, localized Ca^{2+}-release events arising at the nuclear poles were of similar amplitude to Ca^{2+} sparks, but often exhibited a plateau phase of variable duration (Fig. S1).

The Golgi apparatus is consistently present at the nuclear poles in ARVMs, where it appears as a series of flattened membranous sacs in electron micrographs (Fig. S2*A*). In this example, localization of the Golgi at one nuclear pole was highlighted by DAB staining of the Golgi matrix protein GM130. The *cis* face of the Golgi apparatus was in close apposition to the nuclear envelope, while the *trans* face was bounded by mitochondria. Using confocal microscopy, expression of GFP targeted to the Golgi apparatus identified the organelle at the nuclear poles and also Golgi transfer vesicles within the cytosol (Fig. S2*B*, *left*). Pre-exposure of GFP expressing cells to the selective Golgi disrupting agent ilimaquinone (IQ)20 resulted in complete loss of both the Golgi apparatus at the nuclear poles and the transfer vesicles (Fig. S2*C*, *right*). Given the consistent presence of the Golgi apparatus at the nuclear poles in ARVMs, experiments were carried out to establish whether the prolonged Ca^{2+}-release events co-localize with the organelle.

Cells were co-loaded with Golgi-ID green to identify the Golgi apparatus, and fluo-4 to detect changes in cytosolic Ca^{2+} concentration. An initial x-y confocal image revealed both the location of the Golgi apparatus and the evenly distributed cytosolic fluo-4 signal (Fig. 1*B*, *left*). The x-y image was then used to position the scan line through the Golgi apparatus at both ends of the nucleus and several bright cytosolic vesicles (Fig 1*B*, *broken line*). On initiation of the line scan, the Golgi apparatus was initially highlighted as a series of bright horizontal lines corresponding to the Golgi-ID green signal (Fig. 1*B*, *middle*). However, because Golgi-ID green bleaches rapidly (Fig. S3), cytosolic fluo-4 fluorescence was left as the remaining stable component of the signal (Fig. 1*D*, *right*). The prolonged Ca^{2+}-release events at the nuclear poles consistently aligned with the Golgi-ID signal. Co-localization of prolonged Ca^{2+}-release with cytosolic vesicles did not typically occur.

Prolonged Ca^{2+}-release events are abolished by selective Golgi disruption

The possibility that the Golgi apparatus is the source of the prolonged Ca^{2+}-release events was investigated further by using IQ to disrupt the organelle. Confocal imaging was carried out in fluo-4 loaded ARVMs, with the scan line positioned longitudinally through the poles of at least one nucleus. In cells initially exhibiting repetitive Ca^{2+}-release events (Fig. 2*A*), exposure to IQ abolished Ca^{2+}-release. In contrast, IQ had no influence on SR Ca^{2+} regulation, as indicated by a lack of effect on the amplitude of the caffeine-induced Ca^{2+}

transient (Fig. 2*B*), the frequency or amplitude of spontaneous SR Ca^{2+} waves (Fig. 2*C*), or the properties of localized SR Ca^{2+} sparks (Fig. 2*D*). Both the location of the prolonged Ca^{2+}-release events and their selective abolition with IQ indicate that the site of origin is the Golgi apparatus. Therefore, prolonged Ca^{2+}-release events arising at the nuclear poles will now be referred to as Golgi Ca^{2+}-release.

Golgi Ca^{2+} release arises from a Ca^{2+} pool that is distinct from the SR

Experiments were done to characterize the properties of Golgi Ca^{2+} release and its relationship to Ca^{2+}-release from the SR. Cell permeabilization allowed the cytosolic conditions to be adjusted, such that regular spontaneous SR Ca^{2+} waves could be induced. A line-scan image was obtained from a permeabilized cell, with the scan line positioned longitudinally through both nuclei (Fig. 2*E*, *upper left*). The image shows a Golgi Ca^{2+} release event that originated close to one end of the lower nucleus. In this example, an SR Ca^{2+} wave arose spontaneously in the middle of the cell during the Golgi Ca^{2+} release (Fig. 2*E*, *arrow*), before propagating in both directions to the ends of the myocyte. The SR Ca^{2+} wave added to the Golgi Ca^{2+}-release event, but did not affect the underlying time course (Fig, 2*E*, *upper right*), providing strong evidence that the SR and Golgi Ca^{2+} stores are not interconnected.

Another consistent feature was that Golgi Ca^{2+} release diffused further into the nucleoplasm than the cytosol (Fig. 2*E*, *lower right*). This might be explained by the close proximity of the trans-Golgi apparatus to mitochondria (Fig S2), which acts as a Ca^{2+} sink. Inhibition of mitochondrial Ca^{2+} uptake with RU360 was found to stimulate GCR (Fig. S4). This is likely due to Ca^{2+} loss from the mitochondria and consequent effects in the Golgi Ca^{2+} uptake/release.

Further experiments provided evidence of a limited interaction between SR Ca^{2+}-release and CGR. In the line-scan image shown in Fig. 2*F*, a spontaneous SR Ca^{2+} wave arose close to the center of a permeabilized cell (*arrow*) and then propagated in both directions to the ends of the cell. In this example, the SR Ca^{2+} wave triggered a prolonged Golgi Ca^{2+} release originating at the pole of one nucleus. Again, this event exhibited a typical plateau phase and a local increase in both cytosolic and nucleoplasmic Ca^{2+} concentration was apparent.

A similar interplay between SR Ca^{2+}-release and Golgi Ca^{2+} release was observed in intact myocytes. Fig. 2*G* shows Golgi Ca^{2+} release originating close to one end of the lower nucleus. The cell was then field stimulated during the plateau phase and as shown by the line profile (*lower right*), this form of global SR Ca^{2+}-release also had no detectable influence on the amplitude or time course of Golgi Ca^{2+} release. However, the global SR Ca^{2+}-release triggered Golgi Ca^{2+} release at one pole of the other nucleus (*upper right*).

Golgi apparatus Ca^{2+} release involves RyRs

A number of interventions were carried out to investigate the mechanisms underlying Ca^{2+} uptake and-release from the Golgi apparatus (Table 1). In permeabilized cells perfused with a mock intracellular solution containing 120 nM free Ca^{2+} concentration, 17.6% of myocytes exhibited Golgi Ca^{2+} release during a standardized 3 minute line scan. Lowering the free Ca^{2+} concentration decreased, while raising significantly increased the percentage

of cells exhibiting Golgi Ca^{2+} release. In intact ARVMs, pre-incubation with ryanodine at a concentration that blocks RyR2 in its closed state abolished Golgi Ca^{2+} release, as did pre-incubation with the SERCA inhibitor thapsigargin. These findings suggest that RyR Ca^{2+} efflux and SERCA mediated Ca^{2+} uptake have a major role in Golgi Ca^{2+} regulation in ARVMs.

$InsP_3$ can induce depletion of Golgi apparatus luminal Ca^{2+} in various cell types3,13–15. In addition, studies on mouse myocytes have provided evidence that endothelin-1 (ET-1: which increases [$InsP_3$]) or InsP3R agonists, can induce Ca^{2+} efflux from the closely apposed nuclear envelope21. However, in the present study ET-1 did not stimulate Golgi Ca^{2+} release in intact ARVMs and the InsP3R blocker 2-APB had no significant effect on the percentage of cells exhibiting Golgi Ca^{2+} release under basal conditions. Similarly, in permeabilized myocytes, the $InsP_3R$ agonist adenophostin-A did not stimulate Ca^{2+}-release at the nuclear poles.

The β_1-adrenergic pathway modulates Golgi Ca^{2+} release

β_1-adrenergic signaling has major effects on SR Ca^{2+} regulation, which involve a rise in cAMP concentration and activation of both PKA and Epac pathways22,23. Therefore, experiments were carried out to establish whether β_1-adrenoceptor activation also stimulates Golgi Ca^{2+} release in intact ARVMs. In this series of experiments, 11.4 % of intact ARVMs under control conditions. In the presence of 20, 100 and 1000 nM isoproterenol, the percentage of cells exhibiting Golgi Ca^{2+} release increased to 13%, 23.3% and 26.3% respectively (Fig. 3*A*).

This relatively small effect of isoproterenol on Golgi Ca^{2+} release might be explained if the cAMP concentration is low in the vicinity of the Golgi apparatus, for example, due to local PDE activity. Consistent with this, in the presence of only 10 nM isoproterenol, which did not itself influence Golgi Ca^{2+} release, the non-specific PDE inhibitor IBMX increased the percentage of cells exhibiting Golgi Ca^{2+} release to 55% (Fig. 3*A*). The selective PDE2 inhibitor EHNA had no significant effect with or without isoproterenol. However, in the presence of 5 or 10 nM isoproterenol, PDE3 inhibition with milrinone increased the percentage of cells exhibiting Golgi Ca^{2+} release to 80% and 83.3% respectively. Inhibition of PDE4 with rolipram increased the percentage of cells exhibiting Golgi Ca^{2+} release to 72.7% and 100% (Fig. 3*A*). Inhibition of PDE 3 or 4 typically induced repetitive Golgi Ca^{2+} release, and on average, rolipram or milrinone increased the frequency of Golgi Ca^{2+} release >10 fold relative to isoproterenol alone (Fig. 3 *B*&*C*). PDE 3 or 4 inhibition also increased Golgi Ca^{2+} release amplitude relative to isoproterenol alone (Fig. 3*D*).

The influence of isoproterenol and PDE inhibition on Ca^{2+} regulation by the SR was also studied to allow comparison with Golgi Ca^{2+} regulation. In the absence of isoproterenol, rolipram increased spark frequency by 28.6% ± 24.1, although this was not statistically significant (Fig. 3*E*). Milrinone increased spark frequency by 55 ± 20.8%. isoproterenol (10 nM) increased spark frequency by 144.4 ± 28.8%, while addition of isopproterenol with rolipram or milrinone increased spark frequency by 215.7 ± 38.2% and 297.2 ± 29.63% respectively. Rolipram or milrinone alone had no significant effect on Ca^{2+} spark amplitude, while isoproterenol significantly increased spark amplitude by 9.8 ± 1.41 % (Fig. 3*F*).

Unexpectedly, however, in the presence of isoproterenol+rolipram or isoproterenol +milrinone, spark amplitude was not significantly different to control values. There was a trend towards reduced spark duration, although this was only significant with isoproterenol alone (Fig. 3*G*).

Assessment of the SR Ca^{2+} content with caffeine also revealed differences between the effects of isoproterenol and PDE 3 or 4 inhibition (Fig. 3*H*). Application of isoproterenol alone increased the SR Ca^{2+} content to 121.9 ± 2.68%. However, with isoproterenol combined with PDE 3 or 4 inhibition, the SR Ca^{2+} content was not significantly different to control, consistent with an increased Ca^{2+} leak from the SR.

Both Epac and PKA activation are required for stimulation of Golgi Ca^{2+} release

The SR Ca^{2+} leak that occurs in the presence of isoproterenol is partly due to activation of the Epac pathway and subsequent modification of RyR function by CaMKII22. Therefore, the apparent ability of PDE 3 or 4 inhibition to increase the RyR2 mediated Ca^{2+} leak (Fig. 3*H*) might be explained if a local increase in [cAMP] increases Epac activation.

In ARVMs, the selective Epac activator 8-CPT alone failed to increase the proportion of cells exhibiting Golgi Ca^{2+} release above the basal level (Fig. 3*I*). However, in the presence of 2 nM, 8-CPT increased the proportion of cells exhibiting Golgi Ca^{2+} release to 76.9 %. This level of isoproterenol was used to ensure that PKA activation was minimized, while still producing the effect. This effect of 8-CPT was blocked by the CaMKII inhibitor KN93 or by the phospholipase-C (PLC) inhibitor U73122. Line-scan images of a cell under control conditions and immediately after exposure to 8-CPT+isoproterenol, where both sparks and Golgi Ca^{2+} release are apparent, are shown (Fig. 3*J*). Relative to 8-CPT alone, addition of 8-CPT+isoproterenol increased Golgi Ca^{2+} release frequency ~3 fold, while isoproterenol alone had no significant effect (Fig. 3*K*). However, relative to 8-CPT alone, isoproterenol did significantly increase Golgi Ca^{2+} release amplitude, and this further increased in the presence of 8-CPT+isoproterenol (Fig. 3*L*); an effect is consistent with facilitation of Golgi Ca^{2+} uptake.

The effects of Epac activation on Ca^{2+} sparks and the SR Ca^{2+} content were also studied, with 8-CPT added either in the presence or absence of 2 nM isoproterenol. In contrast to the lack of effect on Golgi Ca^{2+} release, 8-CPT alone increased Ca^{2+} spark frequency to 210.2 ± 25.4 of the control value (Fig. 3*M*). Isoproterenol also increased spark frequency to 261.01 ± 32.20% of the control value and this effect was significantly greater than that of 8-CPT alone. However, the combined addition of 8-CPT and isoproterenol had no additional potentiating effect on spark frequency.

The effects on Ca^{2+} spark amplitude reveal differences between the effects of 8-CPT and isoproterenol on the SR; 8-CPT significantly decreased, while isoproterenol increased Ca^{2+} spark amplitude (Fig 3*N*). Furthermore, when 8-CPT and isoproterenol were added in combination, the net effect was an increase in Ca^{2+} spark amplitude, which was significantly greater than with isoproterenol alone. 8-CPT alone had no effect on duration, while isoproterenol significantly abbreviated Ca^{2+} sparks (Fig. 3*O*). When isoproterenol+8-CPT were added, Ca^{2+} spark duration was not significantly different to control. As previously

described22, the differing effects of 8-CPT and isoproterenol on SR Ca^{2+} spark properties likely reflect changes in SR Ca^{2+} content; 8-CPT significantly reduced, while isoproterenol significantly increased the SR Ca^{2+} content (Fig. 3*P*). However, when isoproterenol was added with 8-CPT, the SR Ca^{2+} content was higher than control. The effects of 8-CPT on Ca^{2+} sparks and the SR content are consistent with previous reports24.

If the Golgi is similarly affected, the combined effect of Epac acting on the RyR and a sustained increase in Golgi Ca^{2+} content may both be necessary for stimulation of Golgi Ca^{2+} release (Fig. 3*I*). Consistent with this possibility, 6-Bnz-cAMP, which activates PKA but not Epac, increased SR Ca^{2+} spark frequency (Fig. S5 *A& B*) and the SR Ca^{2+} content (Fig. S5 *C*) but failed to stimulate Golgi Ca^{2+} release (Fig. S5*D*).

It has been suggested that β_1-adrenergic stimulation can cause an increase in [NO], which activates an RyR2 mediated Ca^{2+} leak25. However, experiments involving measurement of NO with DAF-2 failed to detect a significant increase in NO following a 12 minute exposure to a supramaximal dose of isoproterenol in ARVMs, (Fig. S6 *A & B*). As a positive control, the NO donor GSNO did increase NO. The nitric oxide synthase (NOS) inhibitor L-NAME failed to block the stimulating effect of isoproterenol on Golgi Ca^{2+} release, or SR Ca^{2+} spark parameters (Fig. S6, *C-G*). These data suggest that NO does not have a major role in the stimulating effect of β_1-adrenoceptor activation on Ca^{2+} sparks, or Golgi Ca^{2+} release in ARVMs.

Heart failure is associated with enhanced β_1-adrenergic stimulation of Golgi Ca^{2+} release

Expression of PDE3 and 4 is reportedly decreased in heart failure, which might, therefore, lead to β_1-adrenergic facilitation of Golgi Ca^{2+} release in the absence of pharmacological agents. Therefore, the response to β_1-adrenoceptor stimulation was investigated in the monocrotaline model of right heart failure26. Right heart failure was associated with a marked reduction in expression of PDE3A, PDE4A, PDE4B and PDE4D (Fig 4*A*). In ARVMs from heart failure animals 20 nM isoproterenol caused only a small increase in SR Ca^{2+} spark frequency, while spark amplitude and the amplitude of the electrically stimulated Ca^{2+} transient did not change significantly (Fig. 4*B*). This contrasts with controls, where spark frequency, spark amplitude and twitch amplitude all increased significantly, consistent with the previously reported blunting of the β_1-adrenergic response in MCT induced heart failure27. However, unlike the effects on SR Ca^{2+} regulation, isoproterenol markedly increased the percentage of heart failure cells exhibiting Golgi Ca^{2+} release ($n=6$, $p<0.05$). This suggests that despite blunting of the β_1-adrenergicresponse, downregulation of PDE 3 and 4 facilitates the action of cAMP on the Golgi, as acute PDE inhibition does in normal myocytes.

Conditions that promote Golgi Ca^{2+} release facilitate trafficking of VEGFR-1 to the surface membrane

Experiments were carried out to investigate whether conditions that induce Golgi Ca^{2+} release influence trafficking of proteins to the surface membrane, a key role of this organelle. Under control conditions, all ARVMS exhibited a punctate intracellular VEGFR-1 distribution (Fig. 5*A*), which co-localized with the Golgi apparatus resident protein GM130

(Fig. *5B*). When present, the striated VEGFR-1 pattern co-localized with Nav1.1, which is located within the sarcolemma/t-tubules in cardiac cells (Fig 5*C*). However, only 29.1 ± 9.3% of control cells were striated or partially striated, indicating a sarcolemmal/t-tubule VEGFR-1 distribution (Fig 5*D*).

These data suggest that the receptor is primarily localized within the Golgi apparatus at the ends of the nuclei and within cytosolic vesicles under control conditions, but not the sarcolemma. Incubation of ARVMs with isoproterenol, which had no effect on Golgi Ca^{2+} release, failed to influence the cellular distribution of VEGFR-1 (Fig 5*A* & *D*). However, all conditions found to stimulate Golgi Ca^{2+} release (Fig 3) markedly increased the percentage of cells exhibiting a striated VEGFR-1 expression pattern (Fig 5*A* & *D*). As shown for the effect of 8-CPT+ isoproterenol, this effect was also present if the cells were subjected to field stimulation throughout the protocol (Fig. 5*D*). Preincubation of cells with BAPTA-AM to strongly buffer cytosolic [Ca^{2+}] blocked the increase in VEGFR-1 expression at the surface membrane (Fig. 5*D*). These data suggest that stimulation of Golgi apparatus Ca^{2+} cycling facilitates trafficking of VEGFR-1 from the Golgi apparatus to the sarcolemma in ARVMs.

Discussion

The present study shows that prolonged Ca^{2+}-release events arise at the nuclear poles in ARVMs and co-localize with the Golgi apparatus (Fig. 1*B*). Furthermore, IQ-induced disruption of the Golgi apparatus at the nuclear poles (Fig. 2*A*) abolished Golgi Ca^{2+} release, without affecting SR Ca^{2+} regulation (Fig. 2*C-D*). Together, these findings suggest that the prolonged Ca^{2+}-release events at the nuclear poles are the cytosolic consequence of Golgi apparatus Ca^{2+} depletion described in earlier studies on a range of other cell types8,13,14,16. The greater diffusion Ca^{2+} into the nucleus rather than the cytosol (Fig. *2E*) is consistent with the close proximity of the *trans*-Golgi apparatus to mitochondria, which act as a Ca^{2+} sink28 and also the absence of active Ca^{2+} uptake mechanisms within the nucleoplasm. Proximity to mitochondria might also explain why the Golgi apparatus at the nuclear poles is more likely to exhibit Ca^{2+} release than cytosolic vesicles, for example, if mitochondrial Ca^{2+} fluxes influence Golgi Ca^{2+} regulation28.

Golgi Ca^{2+} release involves RyR mediated Ca^{2+} efflux and SERCA Ca^{2+} uptake

In ARVMs, Golgi Ca^{2+} release was abolished by ryanodine. This is consistent with findings in HL-1 cells (which partially retain an adult cardiac phenotype) that functional RyRs are present within the Golgi29. In addition, caffeine-sensitive Ca^{2+} efflux from both the trans and medial Golgi apparatus has been reported in neonatal cardiac and HL-1 cells respectively2,30. These data suggest that in ARVMs, RyRs are an important component of the Golgi Ca^{2+} efflux pathway. Basal Golgi Ca^{2+} release may, therefore, be the equivalent of spontaneous Ca^{2+} sparks.

The luminal Golgi environment in particular differs from that of the SR in that it has calnuc as the major Ca^{2+} buffer9 which unlike calsequestrin, is not known to affect RyR gating. The Ca^{2+} binding protein calumenin is also present within the GA and previous work has shown that it inhibits the direct activating effect of luminal Ca^{2+} on RyR231. It has been

shown that interventions that modify the relationship between RyR2 gating and SR luminal Ca^{2+} can induce long lasting SR Ca^{2+} sparks32. The prolonged nature of Golgi Ca^{2+} release may, therefore, reflect the environment within the Golgi and consequent effects on RyR gating.

In the present study, drugs that increase $InsP_3$ or block $InsP_3Rs$ did not affect Golgi Ca^{2+} release under control conditions. However, PLC and $InsP_3R$ receptor activation are part of the signaling cascade that links Epac activation to CaMKII phosphorylation of RyR2, and an increase in SR Ca^{2+} spark frequency22. As with Ca^{2+} sparks33, PLC inhibition prevented stimulation of Golgi Ca^{2+} release by isoproterenol+8-CPT (Fig. 3*I*). Therefore, $InsP_3R$ activation may either directly (via Ca^{2+} release) or indirectly (via CaMKII) facilitate Golgi Ca^{2+} release when Epac is activated.

In contrast to neonatal cardiac myocytes where Ca^{2+} uptake into the trans-Golgi was exclusively dependent on SPCA12, Golgi Ca^{2+} release was abolished by thapsigargin, implicating SERCA as an important Ca^{2+} uptake mechanism underlying this form of Ca^{2+} release in ARVMs. However, this finding does not exclude the possibility that SPCA1 also contributes to Ca^{2+} uptake in ARVMs.

Golgi apparatus and SR Ca^{2+}-release are functionally independent

One of the most striking findings obtained in the present study was that once initiated, spontaneous or triggered global SR Ca^{2+}-release had no apparent effect on the underlying time course of Golgi Ca^{2+} release (Fig. 2*E-G*). As spontaneous SR Ca^{2+} waves deplete the SR by 80-90%34, it is unlikely that Golgi Ca^{2+} release and Ca^{2+} sparks originate from a common Ca^{2+} pool. Furthermore, previous work on cardiac cells has established (i) that the lumen of the nuclear envelope is contiguous with that of the SR, allowing Ca^{2+} to diffuse freely between both compartments and (ii) that global SR Ca^{2+}-release is associated with rapid (peak ~170 ms) depletion of nuclear envelope Ca^{2+} 35. Therefore, the absence of an effect of global SR Ca^{2+}-release on the underlying time course of Golgi Ca^{2+} release (Fig. 2) excludes the nuclear envelope as a the likely source of Ca^{2+} and is consistent with anatomical and functional separation of the SR and Golgi Ca^{2+} stores. Global SR Ca^{2+}-release did occasionally trigger prolonged Golgi Ca^{2+} release (e.g. Fig. 2*F*). However, this can be explained by the presence of RyR2 within the Golgi apparatus2, which would be expected to exhibit Ca^{2+} induced Ca^{2+}-release.

Golgi Ca^{2+} release is stimulated by activation of the β_1-adrenergic signaling pathway

In the present study, introduction of isoproterenol alone had only a small stimulating effect on Golgi Ca^{2+} release while isoproterenol plus PDE 3 or 4 inhibition markedly stimulated Golgi Ca^{2+} release. This is consistent with compartmentalization of β_1-adrenergic signaling36, such that the cAMP concentration at the Golgi membrane is affected by PDE 3 and 4 activity. In support of this, multiple components of the β_1-adrenergic signaling pathway are associated with scaffolding proteins, which are targeted to specific subcellular locations (Fig. S7). For example, muscle-specific A-kinase anchoring proteins (mAKAPs) form signaling complexes comprising PKA, Epac, PDE 4D3 and protein phosphatase 2A37. mAKAPs are targeted to the nuclear envelope, but are also associated with RyRs in cardiac

myocytes 38,39. In addition, the scaffold protein myomegalin anchors PDE 4D3 to the Golgi apparatus40 and particulate PDE 3 is membrane-bound and also present in the perinuclear region41.

Golgi Ca^{2+} regulation has effects on VEGFR-1 trafficking

It has been shown that both the Ca^{2+} within the Golgi apparatus and local cytosolic Ca^{2+} exert a regulatory influence on the structure of the organelle and on vesicle trafficking2,3,6. The effects of local cytosolic Ca^{2+} may involve Golgi-associated calmodulin-like Ca^{2+} binding proteins (e.g. calneuron1/2, NCS-1), which regulate the activity of phosphatidylinositol 4-OH kinase IIIβ (PI-4Kβ), local synthesis of phospholipids and vesicle trafficking6. β_1-adrenergic signaling also has effects on the function of the Golgi apparatus in a variety of cell types42,43.

The present study provides a plausible link between these two sets of observations; as β_1-adrenergic stimulation can facilitate Golgi Ca^{2+} release (Fig 3), the influence of β_1-adrenergic stimulation on the Golgi apparatus may involve Ca^{2+} dependent regulation. This possibility is supported by the effects on VEGFR-1 localization (Fig. 5). As described in endothelial cells44, VEGFR-1 was located primarily within the Golgi apparatus in ARVMs under control conditions (Fig. 5*B*). However, all factors that facilitated Golgi Ca^{2+} release increased trafficking of VEGFR-1 to the surface membrane (Fig. 5*A* & *D*). This is of is of relevance to work showing that VEGFR-1 is involved in preconditioning, whereby brief periods of intermittent ischemia improve the functional and structural integrity of the heart following subsequent ischemia/reperfusion45. It has been shown that PDE is inhibited during ischemic preconditioning46 and that transient pharmacological PDE inhibition can mimic ischemic preconditioning47. The present work suggests that increased sarcolemmal expression of VEGFR-1, secondary to β_1-adrenoceptor mediated effects on Golgi Ca^{2+}, may contribute to these effects. Moreover, our findings suggest that activation of Epac may provide a novel method to increase sarcolemmal VEGFR-1, thereby facilitating the preconditioning response.

The current findings may also be relevant to work implicating local, rather than global, Ca^{2+} regulation in the control of key cardiac signaling pathways48; β_1-adrenoceptor stimulation is known to induce hypertrophy by a pathway that involves activation of Epac and subsequent effects that involve ‘nuclear factor of activated t-cells’ (NFAT) and/or myocyte enhancer factor 2 (MEF2) transcription factors (Fig S5). 33,49. Both of these pathways are Ca^{2+} regulated, for example, NFAT activation is controlled by the Ca^{2+}/calmodulin-dependent phosphatase calcineurin, which is present at the nuclear poles50. Epac induced activation of $InsP_3$ receptors and consequent effects on nucleoplasmic [Ca^{2+}]/CaMKII are required for the nuclear export of histone deacetylase-5 from the nucleus, which precedes MEF2 activation33. Local Golgi Ca^{2+} release may influence these signaling pathways, particularly during the development of hypertrophy and heart failure, when sustained β_1-adrenergic activation and PDE downregulation occur.

Conclusions

These data establish that the Golgi apparatus is a juxtanuclear focal point for β_1-adrenergic signaling in the myocardium, exhibits functional plasticity under pathological conditions and has the capacity to impose local changes in Ca^{2+} concentration, despite the presence of global cytosolic Ca^{2+} transients that underlie the primary function of the cell. Furthermore, we show that activation of the β_1-adrenergic pathway has distinct effects on Ca^{2+}-release from the Golgi apparatus, which involve local regulation of [cAMP] by PDE 3 and 4, and activation of Epac and PKA, with consequent effects on receptor trafficking.

Materials and Methods

Preparation of cells and solutions

Wistar rats (150-200g) were sacrificed in accordance with the UK Home Office Guidance on the Operation of Animals (Scientific Procedures) Act of 1986. ARVMs were isolated by collagenase digestion as described previously51. Intact myocytes were superfused with solutions containing (mM): 113 NaCl; 5.4 KCl; 1 $MgCl_2$; 1.0 $CaCl_2$; 0.37 Na_2HPO_4; 5.5 glucose; 5 HEPES, pH 7.1. Changes in cytosolic Ca^{2+} concentration were detected by loading the myocytes with fluo-4 AM (5 μM) for 15 minutes at room temperature (20-22°C). In some experiments, cells were permeabilized by exposure to saponin (10 μg/ml) in a mock intracellular solution for 10 minutes, before centrifugation and re-suspension. The intracellular solution contained (mM) 100 KCl; 25 HEPES; 0.36 or 0.05 EGTA; 10 phosphocreatine; 5 ATP and fluo-4 (5 μM), pH 7.0. The free Ca^{2+} and Mg^{2+} concentrations were adjusted to 120 nM and 1 mM respectively by addition of $CaCl_2$ and $MgCl_2$. Unless otherwise stated, all chemicals were obtained from Sigma Aldrich (Dorset, UK). Isoproterenol was obtained from Martindale Pharmaceuticals, Essex, UK. In some experiments the β_2-antagonist ICI 118,551 (100 nM) was included in the solutions, although it was not found to influence the results reported here. The rolipram (10 μM), milrinone (10 μM) and IBMX (10 μM) were added to inhibit PDEs. 8-CPT (10 μM) and 6-Bnz-cAMP (600 μM) used to selectively activate Epac or PKA respectively. Caffeine (20 mM) was rapidly applied to induce a maximal SR Ca^{2+} release. A high level of ryanodine (100 μM) was use to block RyRs in the closed state. Thapsigargin (2.5 μM) was applied to selectively inhibit SERCA. ET-1 (100 μM) was applied to increase InsP3 in ARVMs. 2-APB (10 μM) was applied as a blocker of IP3Rs. Preincubation with IQ (25 μM) was used to completely disrupt the Golgi apparatus (1 hour) or to disrupt Golgi Ca^{2+} release (15 mins). KN93 (1 μM) was used to inhibit CaMKII. U7322 (5 μM) was applied to inhibit PLC. RU360 (5 μM) was used to inhibit mitochondrial Ca^{2+} uptake.

Monocrotaline induced heart failure model

Experiments were approved by the local ethical committee and the United Kingdom Home Office. Male Wistar rats (200 g) received a single intraperitoneal injection of monocrotaline (MCT) to induce right ventricular failure (60 mg/kg in saline) or were injected with an equivalent volume of saline as previously. Animals were weighed weekly for 3 week post-injection and then daily. Ethical approval required that animals were killed upon displaying

clinical signs of right heart failure, for example, dyspnea, cold extremities, lethargy, or any weight loss on consecutive days.

Experimental chamber and Ca^{2+} imaging

The experimental chamber was placed on the stage of a Nikon Diaphot Eclipse TE2000 inverted microscope and the cells were viewed using a 60X water immersion lens (Plan Apo, NA 1.2). In most experiments, cells were imaged in line scan mode using a confocal laser-scanning unit (Bio-Rad, Microradiance 2000, Herts UK) attached to the side port of the microscope. Experiments involving rapid x-y confocal Ca^{2+} imaging utilized an Andor Revolution confocal unit fitted with a Yokogawa-X1 spinning disk running at 30-60 frames per second. All dyes were excited at 488 nm and emitted fluorescence was measured at >515 nm. Image processing and analysis were done using ImageJ (http://rsb.info.nih.gov/ij/) software with plugins that allow automatic detection of localized Ca^{2+}-release in line-scan (https://sites.google.com/site/sparkmasterhome/) or x-y images 52.

Identification of the Golgi apparatus using electron or confocal microscopy

For electron microscopy, the left ventricle from paraformaldehyde treated rat heart was sectioned at 50 μm on a vibrating microtome and incubated in an antibody to the Golgi protein GM130 (mouse) 1:200 (BD Biosciences, Oxford England). Following washing, sections were incubated in biotinylated donkey anti-mouse 1:200, (Invitrogen, Europe) prior to extravidin peroxidase (1:1500; Sigma) and visualisation with diaminobenzidine.

For confocal microscopy (Zeiss LSM700) of fixed cells, myocytes were cultured overnight in the presence of the CellLight Golgi-GFP baculovirus (Invitrogen, Paisley, UK), which expresses a fusion construct of a Golgi apparatus marker (targeted to N-acetylgalactosaminyl transferase-2) and GFP. The culture medium comprised Medium 199 with HEPES and the following added ingredients (mM) 5 creatine; 5 taurine; 2 Na-pyruvate, 2 L-Carnitine. The solution also contained primocin 2μl/ml and insulin 0.1 μM. 6 well plates were laminin coated before addition of myocytes at ~ 25,000 cells/ml. Following culture, cells were fixed (Dulbecco's PBS 4% paraformaldehyde, 20 min) and then permeabilized (0.05% Triton-X 100) before DAPI staining to allow both the Golgi apparatus (488 nm excitation, >515 nm emission) and the nucleus (360 nm excitation, 460 nm emission) to be imaged. Colocalization experiments were carried out using Alexa Fluor 488 labeled mouse anti GM130 (1:10, BD Biosciences), a Nav1.1 rabbit primary (1:25, Alomone Labs), followed by donkey anti-rabbit Alexa Fluor 555 (Invitrogen) and a VEGFR-1 antibody (1:25 BD Systems Ltd) followed by donkey anti-goat Alexa Fluor 488 (1:500, Invitrogen).

In experiments involving changes in VEGFR-1 expression at the surface membrane, cells were exposed to a variety of conditions prior to fixing. This included preinculabtion in BAPTA-AM (2.5 μM) for 15 minutes prior to introduction of isoproterenol (10 nM), isoproterenol plus 8-CPT (10 μM) or isoproterenol plus rolipram (10 μM). In some experiments the cells were electrically field stimulated (0.5 Hz) before and during exposure the drugs.

For visualization of the Golgi apparatus in living cells, myocytes were loaded for 15 minutes with Golgi-ID green (0.5 nmoles/ml, Enzo Life Sciences, Exeter, UK), a membrane

Europe PMC Funders Author Manuscripts

permeant Golgi apparatus marker (excitation 488 nM, emission > 515 nm). The Golgi ID green signal was found to bleach rapidly (Fig. S2). Consequently, co-loading with fluo-4 and Golgi ID green allowed the Golgi apparatus to be identified in x-y confocal images before bleaching of the dye, which left the stable Ca^{2+} sensitive fluo-4 signal within the cytosol (see also Fig. 1*B*).

Immunoblotting

The free right ventricular heart wall was dissected, minced, then homogenised for 4 × 10 s in 2 ml cooled (~10 °C) Laemmli buffer without β-mercaptoethanol [63.5 mM Tris (pH 6.8), 10% glycerol, 2% SDS, protease (Roche Applied Science) and phosphatase (Thermo Scientific Pierce) inhibitor cocktails at maximum power using an Ultra-Turrax T8 hand-held homogeniser. After the final homogenisation step, tubes were centrifuged (2000 g, 10 min at 15 °C) to sediment cell debris and unprocessed material. The supernatant was immediately stored at -20 °C. Protein concentration was determined by bicinchoninic acid assay (Sigma-Aldrich). 5% (v/v) β-mercaptoethanol was added to all samples prior to sodium dodecyl sulphate polyacrylamide gel electrophoresis (SDS-PAGE). Separated proteins were transferred from polyacrylamide gels to polyvinylidene fluoride (PVDF) membranes, after which a standard immunoblotting procedure was employed. The PDE3A antibody was obtained from FabGennix Inc (Frisco, USA) and the PDE4A, 4B and 4D antibodies were a gift from Professor Miles Houslay, University of Glasgow.

Statistics

Results are presented as the mean ± S.E.M. Statistical significance was assessed using a t-test, Chi-squared test or ANOVA as appropriate. Differences between means were considered significant at $p<0.05$. Statistics and graph plotting were done were using Origin software (Microcal, UK).

Supplementary Material

Refer to Web version on PubMed Central for supplementary material.

Funding

This work was funded by grants from the British Heart Foundation and the Wellcome Trust.

References and Notes

1. Pizzo P, Lissandron V, Capitanio P, Pozzan T. Ca^{2+} signalling in the Golgi apparatus. Cell Calcium. 2011; 50:184–192. [PubMed: 21316101]
2. Lissandron V, Podini P, Pizzo P, Pozzan T. Unique characteristics of Ca^{2+} homeostasis of the trans-Golgi compartment. Proc Natl Acad Sci U S A. 2010; 107:9198–9203. [PubMed: 20439740]
3. Micaroni M, Perinetti G, Di Giandomenico D, Bianchi K, Spaar A, Mironov AA. Synchronous intra-Golgi transport induces the release of Ca^{2+} from the Golgi apparatus. Exp Cell Res. 2010; 316:2071–2086. [PubMed: 20420828]
4. Porat A, Elazar Z. Regulation of intra-Golgi membrane transport by calcium. J Biol Chem. 2000; 275:29233–29237. [PubMed: 10871627]
5. Peters C, Mayer A. Ca^{2+}/calmodulin signals the completion of docking and triggers a late step of vacuole fusion. Nature. 1998; 396:575–580. [PubMed: 9859992]

6. Mikhaylova M, Reddy PP, Munsch T, Landgraf P, Suman SK, Smalla KH, Gundelfinger ED, Sharma Y, Kreutz MR. Calneurons provide a calcium threshold for trans-Golgi network to plasma membrane trafficking. Proc Natl Acad Sci U S A. 2009; 106:9093–9098. [PubMed: 19458041]
7. Callewaert G, Parys JB, De Smedt H, Raeymaekers L, Wuytack F, Vanoevelen J, Van Baelen K, Simoni A, Rizzuto R, Missiaen L. Similar Ca^{2+}-signaling properties in keratinocytes and in COS-1 cells overexpressing the secretory-pathway Ca^{2+}-ATPase SPCA1. Cell Calcium. 2003; 34:157–162. [PubMed: 12810057]
8. Van Baelen K, Vanoevelen J, Callewaert G, Parys JB, De Smedt H, Raeymaekers L, Rizzuto R, Missiaen L, Wuytack F. The contribution of the SPCA1 Ca^{2+} pump to the Ca2+ accumulation in the Golgi apparatus of HeLa cells assessed via RNA-mediated interference. Biochem Biophys Res Commun. 2003; 306:430–436. [PubMed: 12804581]
9. Lin P, Yao Y, Hofmeister R, Tsien RY, Farquhar MG. Overexpression of CALNUC (nucleobindin) increases agonist and thapsigargin releasable Ca2+ storage in the Golgi. J Cell Biol. 1999; 145:279–289. [PubMed: 10209024]
10. Rojas P, Surroca A, Orellana A, Wolff D. Kinetic characterization of calcium uptake by the rat liver Golgi apparatus. Cell Biol Int. 2000; 24:229–233. [PubMed: 10816324]
11. Taylor RS, Jones SM, Dahl RH, Nordeen MH, Howell KE. Characterization of the Golgi complex cleared of proteins in transit and examination of calcium uptake activities. Mol Biol Cell. 1997; 8:1911–1931. [PubMed: 9348533]
12. Lin P, Le Niculescu H, Hofmeister R, McCaffery JM, Jin M, Hennemann H, McQuistan T, De Vries L, Farquhar MG. The mammalian calcium-binding protein, nucleobindin (CALNUC), is a Golgi resident protein. J Cell Biol. 1998; 141:1515–1527. [PubMed: 9647645]
13. Pinton P, Pozzan T, Rizzuto R. The Golgi apparatus is an inositol 1,4,5-trisphosphate-sensitive Ca^{2+} store, with functional properties distinct from those of the endoplasmic reticulum. EMBO J. 1998; 17:5298–5308. [PubMed: 9736609]
14. Vanoevelen J, Raeymaekers L, Parys JB, De Smedt H, Van Baelen K, Callewaert G, Wuytack F, Missiaen L. Inositol trisphosphate producing agonists do not mobilize the thapsigargin-insensitive part of the endoplasmic-reticulum and Golgi Ca^{2+} store. Cell Calcium. 2004; 35:115–121. [PubMed: 14706285]
15. Mahieu F, Owsianik G, Verbert L, Janssens A, De Smedt H, Nilius B, Voets T. TRPM8-independent menthol-induced Ca^{2+} release from endoplasmic reticulum and Golgi. J Biol Chem. 2007; 282:3325–3336. [PubMed: 17142461]
16. Missiaen L, Van Acker K, Van Baelen K, Raeymaekers L, Wuytack F, Parys JB, De Smedt H, Vanoevelen J, Dode L, Rizzuto R, Callewaert G. Calcium release from the Golgi apparatus and the endoplasmic reticulum in HeLa cells stably expressing targeted aequorin to these compartments. Cell Calcium. 2004; 36:479–487. [PubMed: 15488597]
17. Vanoevelen J, Raeymaekers L, Dode L, Parys JB, De Smedt H, Callewaert G, Wuytack F, Missiaen L. Cytosolic Ca^{2+} signals depending on the functional state of the Golgi in HeLa cells. Cell Calcium. 2005; 38:489–495. [PubMed: 16122795]
18. Missiaen L, Van Acker K, Parys JB, De Smedt H, Van Baelen K, Weidema AF, Vanoevelen J, Raeymaekers L, Renders J, Callewaert G, Rizzuto R, et al. Baseline cytosolic Ca2+ oscillations derived from a non-endoplasmic reticulum Ca^{2+} store. J Biol Chem. 2001; 276:39161–39170. [PubMed: 11514551]
19. Rambourg A, Segretain D, Clermont Y. Tridimensional architecture of the Golgi apparatus in the atrial muscle cell of the rat. Am J Anat. 1984; 170:163–179. [PubMed: 6147083]
20. Takizawa PA, Yucel JK, Veit B, Faulkner DJ, Deerinck T, Soto G, Ellisman M, Malhotra V. Complete vesiculation of Golgi membranes and inhibition of protein transport by a novel sea sponge metabolite, ilimaquinone. Cell. 1993; 73:1079–1090. [PubMed: 8513494]
21. Wu X, Zhang T, Bossuyt J, Li X, McKinsey TA, Dedman JR, Olson EN, Chen J, Brown JH, Bers DM. Local InsP3-dependent perinuclear Ca^{2+} signaling in cardiac myocyte excitation-transcription coupling. J Clin Invest. 2006; 116:675–682. [PubMed: 16511602]
22. Pereira L, Metrich M, Fernandez-Velasco M, Lucas A, Leroy J, Perrier R, Morel E, Fischmeister R, Richard S, Benitah JP, Lezoualc'h F, et al. The cAMP binding protein Epac modulates Ca^{2+}

sparks by a Ca^{2+}/calmodulin kinase signalling pathway in rat cardiac myocytes. J Physiol. 2007; 583:685–694. [PubMed: 17599964]

23. Pereira L, Cheng H, Lao DH, Na L, van Oort RJ, Brown JH, Wehrens XH, Chen J, Bers DM. Epac2 mediates cardiac beta1-adrenergic-dependent sarcoplasmic reticulum Ca^{2+} leak and arrhythmia. Circulation. 2013; 127:913–922. [PubMed: 23363625]
24. Oestreich EA, Wang H, Malik S, Kaproth-Joslin KA, Blaxall BC, Kelley GG, Dirksen RT, Smrcka AV. Epac-mediated activation of phospholipase C(epsilon) plays a critical role in beta-adrenergic receptor-dependent enhancement of Ca^{2+} mobilization in cardiac myocytes. J Biol Chem. 2007; 282:5488–5495. [PubMed: 17178726]
25. Gutierrez DA, Fernandez-Tenorio M, Ogrodnik J, Niggli E. NO-dependent CaMKII activation during beta-adrenergic stimulation of cardiac muscle. Cardiovasc Res. 2013; 100:392–401. [PubMed: 23963842]
26. Benoist D, Stones R, Drinkhill M, Bernus O, White E. Arrhythmogenic substrate in hearts of rats with monocrotaline-induced pulmonary hypertension and right ventricular hypertrophy. Am J Physiol Heart Circ Physiol. 2011; 300:H2230–H2237. [PubMed: 21398591]
27. Leineweber K, Seyfarth T, Abraham G, Gerbershagen HP, Heinroth-Hoffmann I, Ponicke K, Brodde OE. Cardiac beta-adrenoceptor changes in monocrotaline-treated rats: differences between membrane preparations from whole ventricles and isolated ventricular cardiomyocytes. J Cardiovasc Pharmacol. 2003; 41:333–342. [PubMed: 12605011]
28. Dolman NJ, Gerasimenko JV, Gerasimenko OV, Voronina SG, Petersen OH, Tepikin AV. Stable Golgi-mitochondria complexes and formation of Golgi Ca^{2+} gradients in pancreatic acinar cells. J Biol Chem. 2005; 280:15794–15799. [PubMed: 15722348]
29. George CH, Rogers SA, Bertrand BM, Tunwell RE, Thomas NL, Steele DS, Cox EV, Pepper C, Hazeel CJ, Claycomb WC, Lai FA. Alternative splicing of ryanodine receptors modulates cardiomyocyte Ca2+ signaling and susceptibility to apoptosis. Circ Res. 2007; 100:874–883. [PubMed: 17322175]
30. Wong AK, Capitanio P, Lissandron V, Bortolozzi M, Pozzan T, Pizzo P. Heterogeneity of Ca^{2+} handling among and within Golgi compartments. J Mol Cell Biol. 2013; 5:266–276. [PubMed: 23918284]
31. Sahoo SK, Kim T, Kang GB, Lee JG, Eom SH, Kim dH. Characterization of calumenin-SERCA2 interaction in mouse cardiac sarcoplasmic reticulum. J Biol Chem. 2009; 284:31109–31121. [PubMed: 19740751]
32. Zima AV, Picht E, Bers DM, Blatter LA. Termination of cardiac Ca^{2+} sparks: role of intra-SR [Ca2+], release flux, and intra-SR Ca2+ diffusion. Circ Res. 2008; 103:e105–e115. [PubMed: 18787194]
33. Pereira L, Ruiz-Hurtado G, Morel E, Laurent AC, Metrich M, Dominguez-Rodriguez A, Lauton-Santos S, Lucas A, Benitah JP, Bers DM, Lezoualc'h F, et al. Epac enhances excitation-transcription coupling in cardiac myocytes. J Mol Cell Cardiol. 2012; 52:283–291. [PubMed: 22056318]
34. MacQuaide N, Dempster J, Smith GL. Assessment of sarcoplasmic reticulum Ca^{2+} depletion during spontaneous Ca2+ waves in isolated permeabilized rabbit ventricular cardiomyocytes. Biophys J. 2009; 96:2744–2754. [PubMed: 19348757]
35. Wu X, Bers DM. Sarcoplasmic reticulum and nuclear envelope are one highly interconnected Ca^{2+} store throughout cardiac myocyte. Circ Res. 2006; 99:283–291. [PubMed: 16794184]
36. Zaccolo M, Pozzan T. Discrete microdomains with high concentration of cAMP in stimulated rat neonatal cardiac myocytes. Science. 2002; 295:1711–1715. [PubMed: 11872839]
37. Dodge-Kafka KL, Soughayer J, Pare GC, Carlisle Michel JJ, Langeberg LK, Kapiloff MS, Scott JD. The protein kinase A anchoring protein mAKAP coordinates two integrated cAMP effector pathways. Nature. 2005; 437:574–578. [PubMed: 16177794]
38. Kapiloff MS, Jackson N, Airhart N. mAKAP and the ryanodine receptor are part of a multi-component signaling complex on the cardiomyocyte nuclear envelope. J Cell Sci. 2001; 114:3167–3176. [PubMed: 11590243]
39. Bauman AL, Michel JJ, Henson E, Dodge-Kafka KL, Kapiloff MS. The mAKAP signalosome and cardiac myocyte hypertrophy. IUBMB Life. 2007; 59:163–169. [PubMed: 17487687]

40. Verde I, Pahlke G, Salanova M, Zhang G, Wang S, Coletti D, Onuffer J, Jin SL, Conti M. Myomegalin is a novel protein of the golgi/centrosome that interacts with a cyclic nucleotide phosphodiesterase. J Biol Chem. 2001; 276:11189–11198. [PubMed: 11134006]
41. Kauffman RF, Crowe VG, Utterback BG, Robertson DW. LY195115: a potent, selective inhibitor of cyclic nucleotide phosphodiesterase located in the sarcoplasmic reticulum. Mol Pharmacol. 1986; 30:609–616. [PubMed: 2946929]
42. Mayinger P. Signaling at the Golgi. Cold Spring Harb Perspect Biol. 2011; 3
43. Arakel EC, Brandenburg S, Uchida K, ZHANG H, Lin YW, Kohl T, Schrul B, Sulkin MS, Efimov IR, Nichols CG, Lehnart SE, et al. Tuning the electrical properties of the heart by differential trafficking of KATP ion channel complexes. J Cell Sci. 2014
44. Mittar S, Ulyatt C, Howell GJ, Bruns AF, Zachary I, Walker JH, Ponnambalam S. VEGFR1 receptor tyrosine kinase localization to the Golgi apparatus is calcium-dependent. Exp Cell Res. 2009; 315:877–889. [PubMed: 19162007]
45. Thirunavukkarasu M, Juhasz B, Zhan L, Menon VP, Tosaki A, Otani H, Maulik N. VEGFR1 (Flt-1+/-) gene knockout leads to the disruption of VEGF-mediated signaling through the nitric oxide/heme oxygenase pathway in ischemic preconditioned myocardium. Free Radic Biol Med. 2007; 42:1487–1495. [PubMed: 17448895]
46. Lochner A, Genade S, Tromp E, Opie L, Moolman J, Thomas S, Podzuweit T. Role of cyclic nucleotide phosphodiesterases in ischemic preconditioning. Mol Cell Biochem. 1998; 186:169–175. [PubMed: 9774198]
47. Sanada S, Kitakaze M, Papst PJ, Asanuma H, Node K, Takashima S, Asakura M, Ogita H, Liao Y, Sakata Y, Ogai A, et al. Cardioprotective effect afforded by transient exposure to phosphodiesterase III inhibitors: the role of protein kinase A and p38 mitogen-activated protein kinase. Circulation. 2001; 104:705–710. [PubMed: 11489779]
48. Goonasekera SA, Molkentin JD. Unraveling the secrets of a double life: contractile versus signaling Ca^{2+} in a cardiac myocyte. J Mol Cell Cardiol. 2012; 52:317–322. [PubMed: 21600216]
49. Metrich M, Laurent AC, Breckler M, Duquesnes N, Hmitou I, Courillau D, Blondeau JP, Crozatier B, Lezoualc'h F, Morel E. Epac activation induces histone deacetylase nuclear export via a Ras-dependent signalling pathway. Cell Signal. 2010; 22:1459–1468. [PubMed: 20576488]
50. Santana LF, Chase EG, Votaw VS, Nelson MT, Greven R. Functional coupling of calcineurin and protein kinase A in mouse ventricular myocytes. J Physiol. 2002; 544:57–69. [PubMed: 12356880]
51. Yang Z, Steele DS. Effects of phosphocreatine on SR Ca^{2+} regulation in isolated saponin-permeabilized rat cardiac myocytes. J Physiol. 2002; 539:767–777. [PubMed: 11897848]
52. Steele EM, Steele DS. Automated Detection and Analysis of Ca^{2+} Sparks in x-y Image Stacks Using a Thresholding Algorithm Implemented within the Open-Source Image Analysis Platform ImageJ. Biophys J. 2014; 106:566–576. [PubMed: 24507597]

Europe PMC Funders Author Manuscripts

Europe PMC Funders Author Manuscripts

One Sentence Summary

Golgi apparatus Ca^{2+}regulation and function is controlled by Epac and PKA signaling

Europe PMC Funders Author Manuscripts

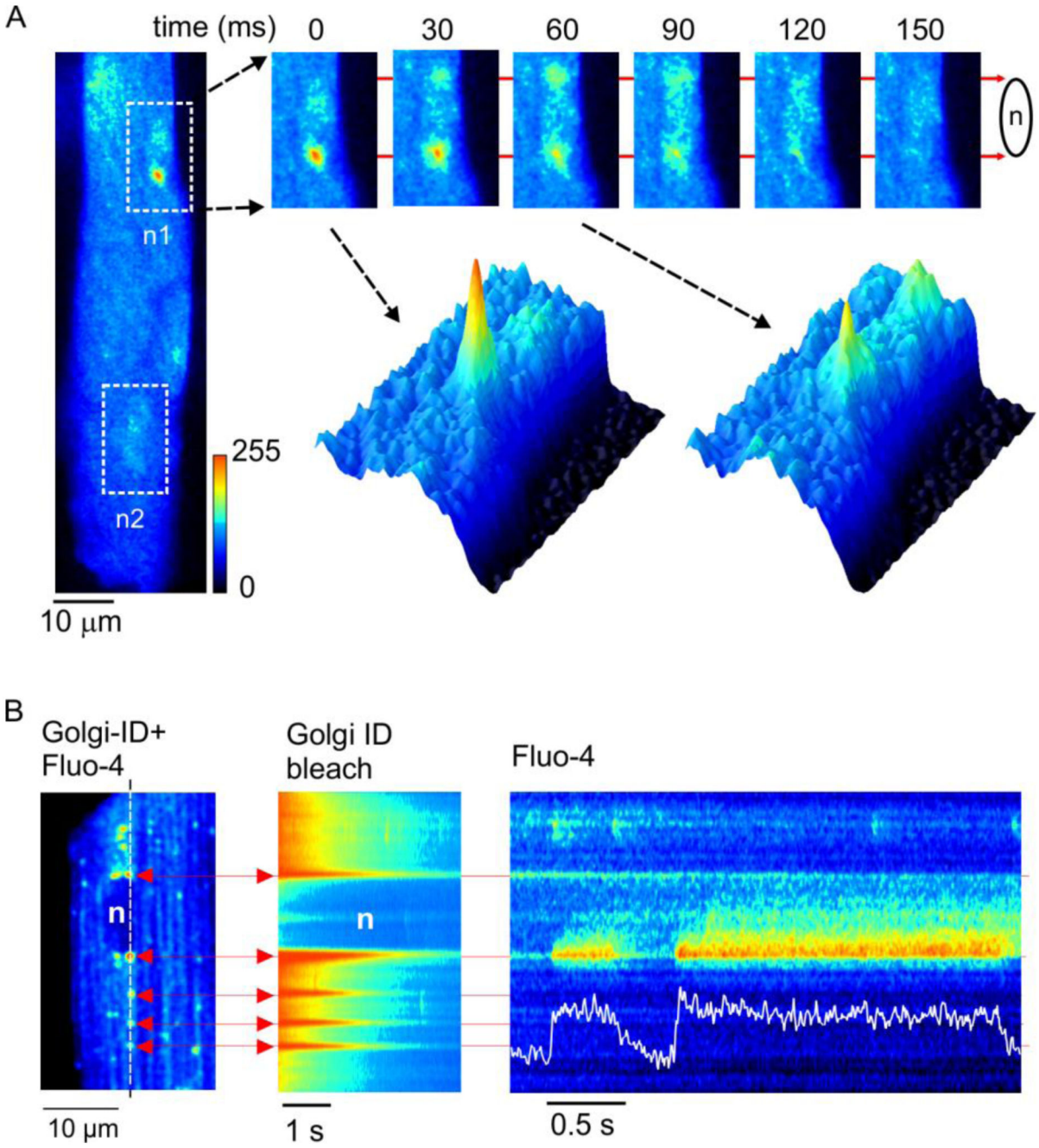

Fig. 1. Prolonged Ca^{2+}-release events co-localize with the Golgi apparatus

(A) x-y confocal images of an intact ARVM. White boxes indicate the location of the 2 nuclei (n1 & n2). **(B)** x-y image showing dual loading of a myocyte with fluo-4 and Golgi-ID (*left*). Diffuse fluorescence reflects cytosolic fluo-4, punctuate fluorescence highlights the Golgi apparatus at the ends of the nucleus and also cytosolic vesicles. Similar effects were seen in cells from 4 hearts.

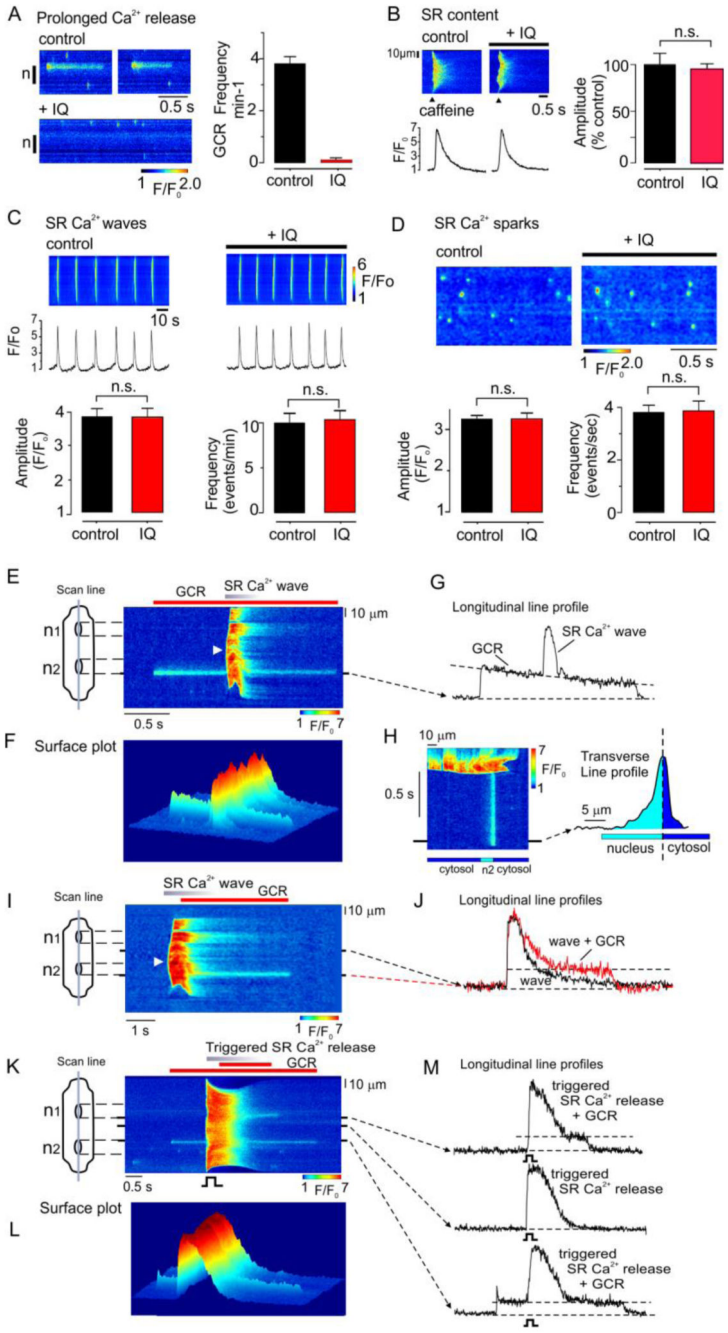

Fig. 2. IQ inhibits Golgi Ca^{2+} release but not SR Ca^{2+}-release

(A) Line scan (*left*) and mean data (*right*) showing that in cells initially exhibiting repetitive Golgi Ca^{2+} release, a subsequent 15 minute exposure to IQ (laser off) abolished Golgi Ca^{2+} release (n=26 cells from 3 hearts). **(B)** original line scan (left) and mean data (right) showing that IQ had no significant effect on the SR Ca^{2+} content assessed as assessed by rapid application caffeine (n=6 cells from 3 hearts) **(C)** Original line scan (*upper*) and mean data (*lower*) showing that IQ has no significant effect on spontaneous SR Ca^{2+} wave amplitude or frequency.(n=8 cells from 3 hearts) **(D)** Original line scan (*upper*) and mean data (*lower*)

showing absence of effect of IQ had on the frequency or amplitude of spontaneous Ca^{2+} sparks (n=8 cells from 3 hearts). * $p<0.05$. n.s., not significant. **(E)** A line scan image (*upper left*) and corresponding surface plots (*lower left & right*) obtained from a permeabilized ARVM in which a spontaneous SR Ca^{2+} wave occurred during a prolonged Ca^{2+}-release event. The line profile is positioned through the prolonged Ca^{2+}-release event (*upper right*). A surface plot orientated from the direction of the arrow *(lower right)* and the accompanying line profile (*right*) indicates diffusion of Ca^{2+} . **(F)** A line scan image showing an SR Ca^{2+} wave originating near the center of a permeabilized cell *(arrow)* triggered a prolonged Ca^{2+}-release event from the upper pole of n2 *(left)* and associated line profiles *(right).* **(G)** A line scan image from an intact myocyte showing a global SR Ca^{2+}-release induced by field stimulation, during a prolonged Ca^{2+}-release event originating from one end of n2. In E-G, similar results were obtained in cells from 2-3 hearts.

Europe PMC Funders Author Manuscripts

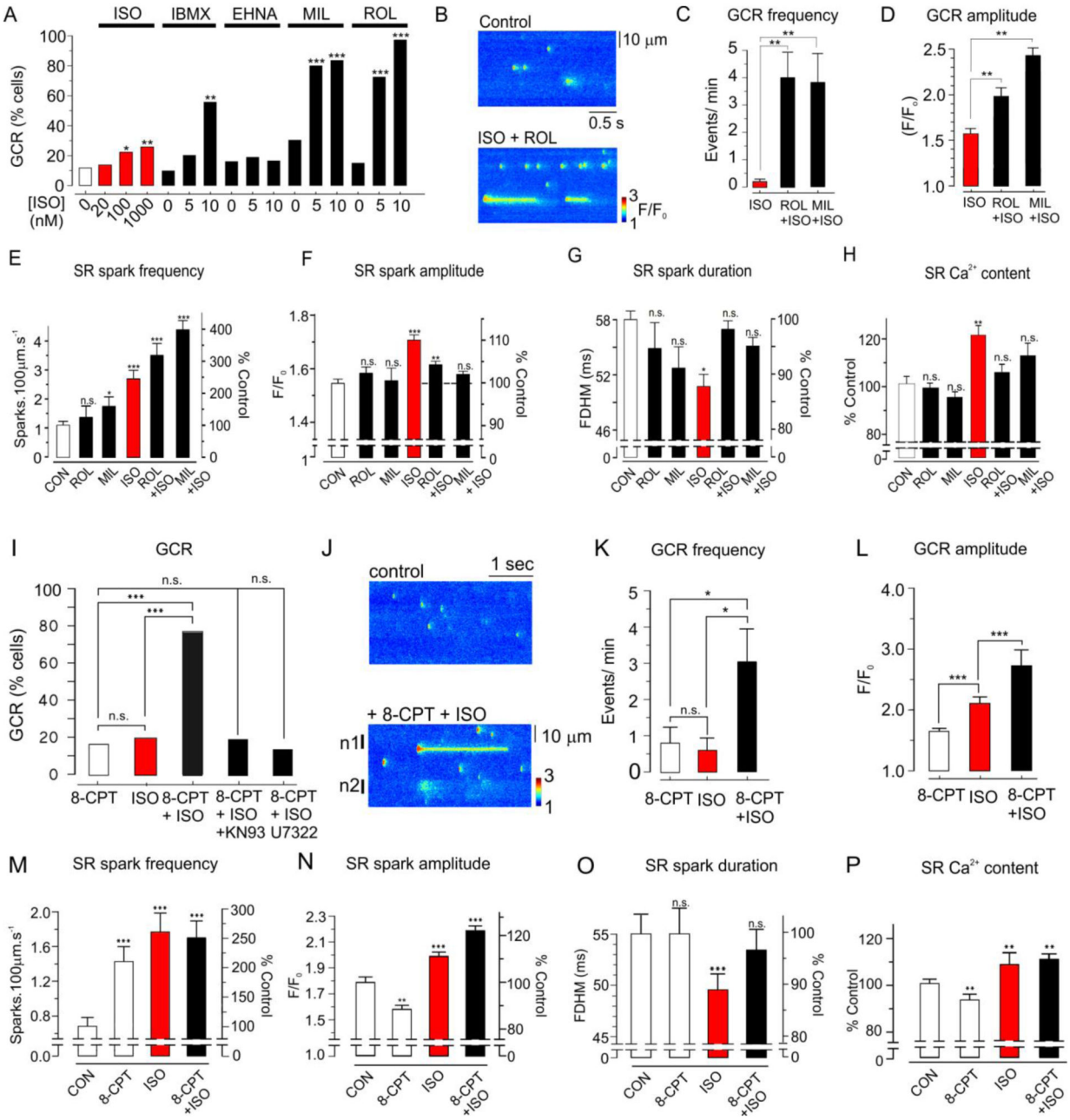

Fig. 3. Stimulation of Golgi Ca^{2+} release by the β_1-adrenergic signaling pathway

(A) Effects of isoproterenol (ISO) (20-1000 nM) or ISO (0, 5 or 10 nM) plus IBMX, EHNA, milrinone (MIL) or rolipram (ROL) on the percentage of cells exhibiting Golgi Ca^{2+} release within a 3 minute line-scan (n=22-30 cells). **(B)** Line-scan of ARVM under control conditions and after introduction of ISO (plus ROL. **(C)** Effects of ROL or MIL + 10 nM ISO on Golgi Ca^{2+} release frequency (n=12-21 cells). **(D)** Effects of PDE 3 or 4 inhibition on Golgi Ca^{2+} release amplitude relative to 10 nM ISO alone (n=12-30 cells). **(E-G)** Effects of ROL, MIL, ISO, ROL+ISO and MIL+ISO on SR Ca^{2+} spark frequency, amplitude (F/F_0),

and full duration at half maximum width (FDHM, n=13-25 cells). **(H)** Effects of ROL, MIL, ISO, ROL+ISO on the SR Ca^{2+} content assessed by application of caffeine (n=8 cells). **(I)** Effect of 8-CPT, ISO , 8-CPT+ISO, 8-CPT+ISO +KN93 and 8-CPT+ISO +U7322 on the percentage of cells exhibiting Golgi Ca^{2+} release (n=10-13 cells) **(J)** line-scan images before and after introduction of 8-CPT+ISO. **(K)** Effects of 8-CPT, ISO and ISO+8-CPT on Golgi Ca^{2+} release frequency (n=10-12 cells). **(L)** Effects of 8-CPT, ISO and ISO+8-CPT on Golgi Ca^{2+} release amplitude (n=10-12 cells). **(M)** Effects of 8-CPT, ISO and ISO+8-CPT on SR Ca^{2+} spark frequency relative to the mean control level (n=15-23 cells). **(N)** Effects of 8-CPT, ISO and ISO + 8-CPT on spark amplitude. **(O)** Effects of 8-CPT, ISO and ISO+8-CPT on Ca^{2+} spark duration (n=22-58 cells). **(P)** Effects of 8-CPT, ISO and ISO+8-CPT on the SR Ca^{2+} content, assessed by rapid application of caffeine (n=10-11 cells). In A-H data was obtained from 3-5 hearts per protocol. In I-P, data was obtained from 3-4 hearts per protocol. *p<0.05, ** p<0.01, ***, p<0.005.

Europe PMC Funders Author Manuscripts

Europe PMC Funders Author Manuscripts

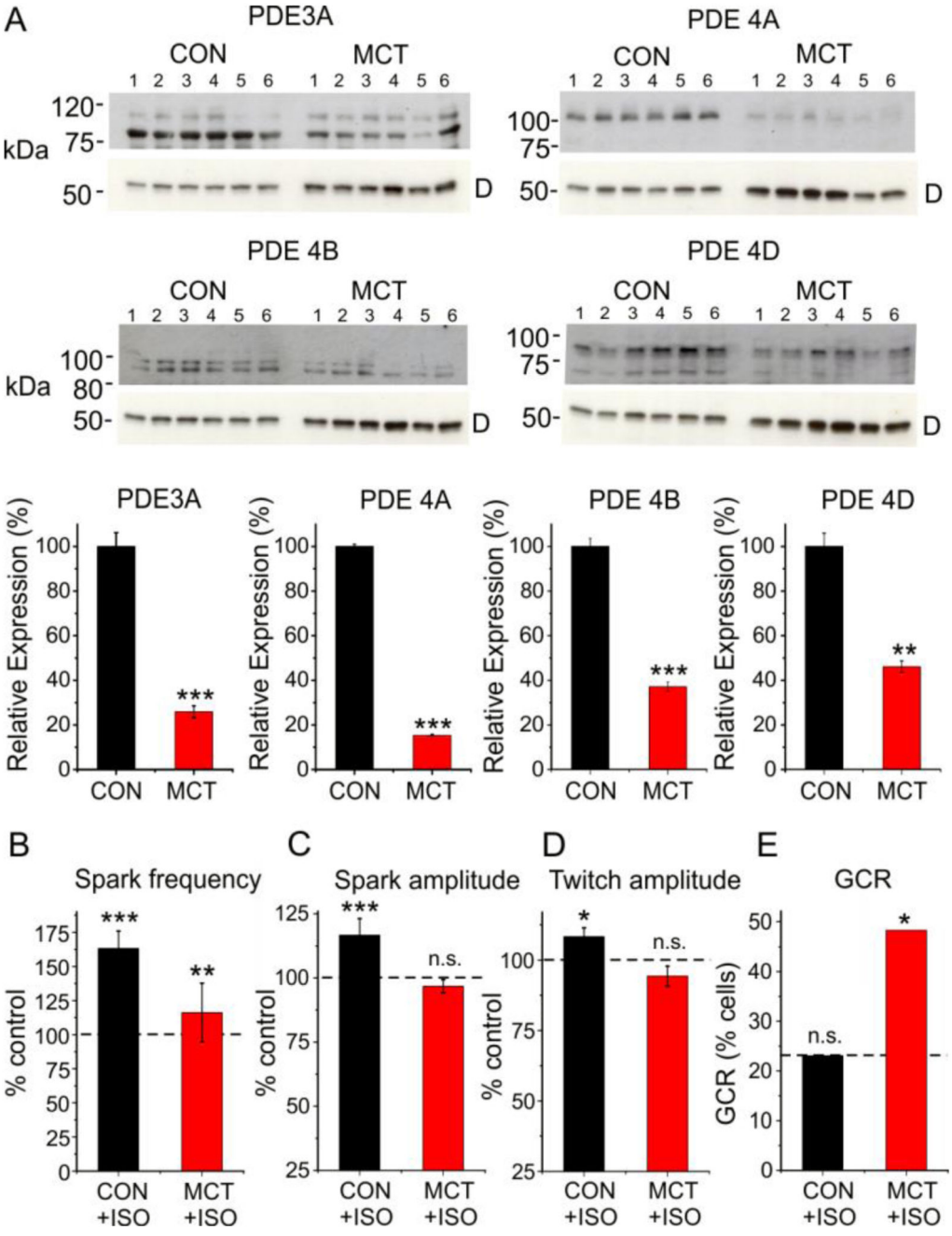

Fig. 4. Changes in PDE expression and Ca^{2+} regulation in heart failure

(A) Western blot data obtained from the hearts of 6 control and 6 MCT-induced heart failure animals (*upper*) and corresponding mean data (*lower*) showing PDE 3A, 4A, 4B and 4D expression. 'D' indicates band corresponding to desmin at ~ 50 kDa. The data were normalized to desmin expression. **(B)** Mean data showing changes in spark frequency, spark amplitude, twitch amplitude and the percentage of cells exhibiting Golgi Ca^{2+} release following exposure to 20 nM ISO in control. For each condition, data were obtained from 22-29 cells from 5 control and 6 MCT hearts. *p<0.05, ** p<0.01, ***, p<0.005.

Europe PMC Funders Author Manuscripts

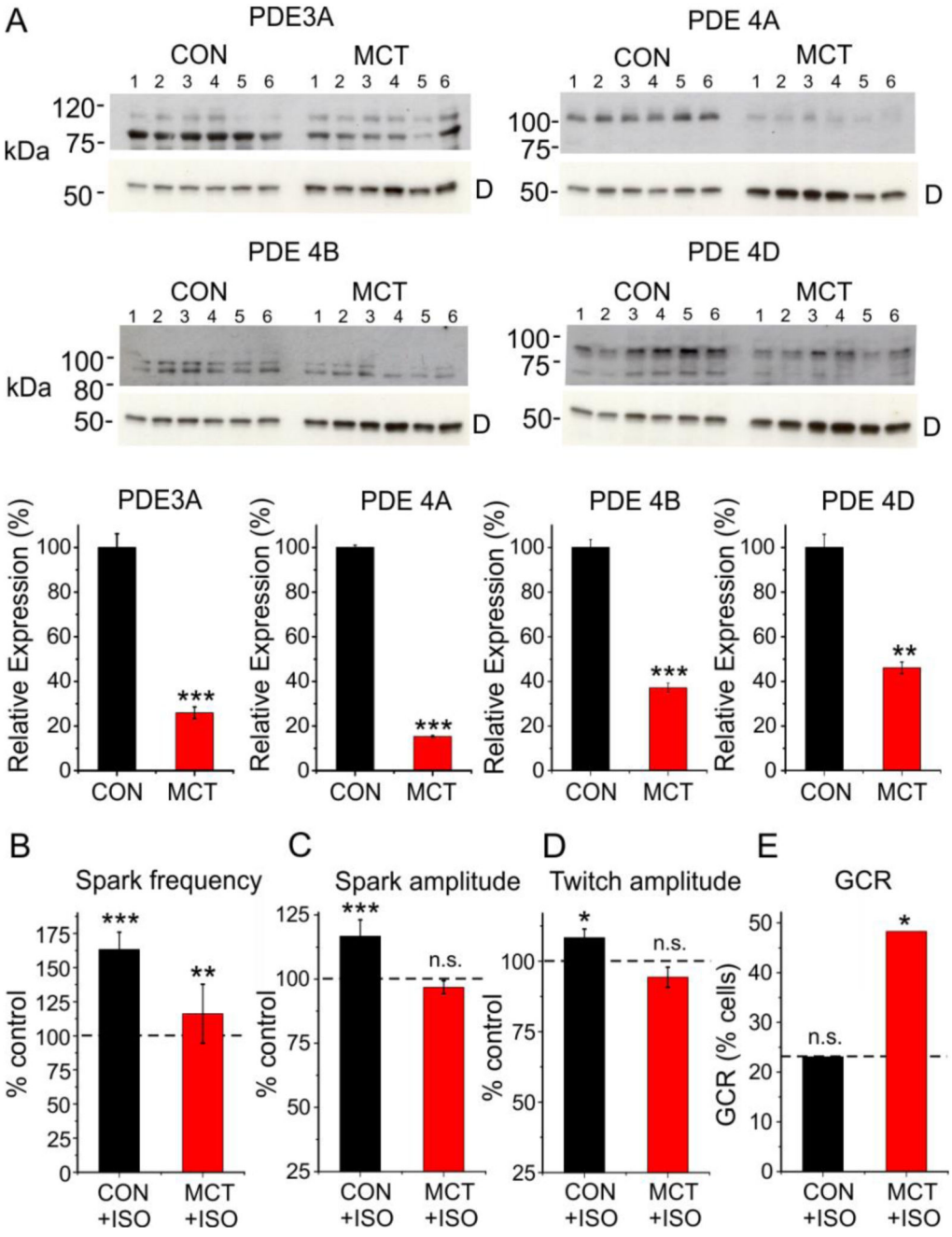

Fig. 5. Conditions that promote Golgi Ca^{2+} release facilitate trafficking of VEGFR-1 to the sarcolemma

(A) Representative immunofluorescence data showing VEGFR-1 expression under control conditions or following exposure to 10 nM ISO, ISO + 8-CPT or ISO + ROL. Line profiles (inset) indicate the presence or absence of striations, indicating sarcolemmal localization. **(B)** Representative images showing intracellular VEGFR-1 (green) and GM130 (red) co-localization (yellow). **(C)** When present, VEGFR-1 striations (green) co-localized with Nav1.1 at the sarcolemma/t-tubules. Line profiles (inset) highlight coincident VEGFR1 and

Nav1.1 peak fluorescence intensities. **(D)** Cumulative data showing percentage of cells exhibiting VEGFR1 striated pattern in the presence of ISO, ISO+ ROL, ISO+MIL and 8-CPT+ISO. Also shown is cumulative data from experiments for similar experiments done during constant field stimulation (stim), field stimulation and ISO+8-CPT or following preincubation in BAPTA-AM. n=60-160 cells from 3-8 hearts. * $p<0.05$. Bar indicates 4 μm.

Europe PMC Funders Author Manuscripts

Europe PMC Funders Author Manuscripts

Table 1

Modulation of Golgi Ca^{2+} release in permeabilized and intact ARVMs

Confocal line scan imaging was used to assess the effect of various interventions on Golgi Ca^{2+} release in permeabilized or intact ARVMs. In permeabilized cells, lowering the Ca^{2+} concentration from the control level of 120 nM to 70 nM significantly reduced, while raising to 250 nM significantly increased the percentage of cells exhibiting Golgi Ca^{2+} release (n=31). Adenophostin-A had no significant effect on Golgi Ca^{2+} release. In intact ARVMs, after treatment with ryanodine or thapsigargin Golgi Ca^{2+} release was never observed. Neither ET-1 nor 2-APB had a significant effect on Golgi Ca^{2+} release. Data were obtained from 3-6 hearts per intervention.

	Permeabilized ARVMs			**Intact ARVMs**			
Intervention	**[Ca^{2+}] 70 nM**	**[Ca^{2+}] 250 nM**	**adenophostin-A**	**ryanodine**	**thapsigargn**	**ET-1**	**2-APB**
Relative change	↓	↑	–	abolished	abolished	–	–
n	n=31	n=31	n=57	n=10	n=10	n=47	n=60
p value	<0.05	<0.005	>0.05	<0.05	<0.05	>0.05	>0.05